Sleep-waking discharge of ventral tuberomammillary neurons in wild-type and histidine decarboxylase knock-out mice

Kazuya Sakai*, Kazumi Takahashi†, Christelle Anaclet and Jian-Sheng Lin

INSERM U628, Claude Bernard University Lyon 1, Lyon, France

Using extracellular single-unit recordings, we have determined the characteristics of neurons in the ventral tuberomammillary nucleus (VTM) of wild-type (WT) and histidine decarboxylase knock-out (HDC-KO) mice during the sleep-waking cycle. The VTM neurons of HDC-KO mice showed no histamine immunoreactivity, but were immunoreactive for the histaminergic (HA) neuron markers adenosine deaminase and glutamic acid decarboxylase 67. In the VTM of WT mice, we found waking (W)-specific, non-W-specific W-active, sleep-active, W and paradoxical sleep (PS)-active, and state-indifferent neuron groups. We previously demonstrated in WT mice that only W-specific neurons are histaminergic and that they are characterized by a triphasic broad action potential. In the VTM of HDC-KO mice, we found all these groups of state-dependent and state-indifferent neurons, including W-specific neurons that were characterized by a triphasic broad action potential and a W-specific slow tonic discharge, as in WT mice. The W-specific neurons ceased firing before the onset of electroencephalogram (EEG) synchronization, the first EEG sign of sleep, and remained silent during both slow-wave sleep (SWS) and PS. At the transition from SWS to W, they discharged after the onset of EEG activation, the first EEG sign of W. They either responded to an arousing stimulus with a long delay or did not respond. They therefore presented exactly the same characteristics as those seen in the VTM of WT mice. Thus VTM neurons deprived of their natural transmitter histamine still exhibit the firing properties of W-specific HA neurons.

Keywords: histamine neurons, tuberomammillary nucleus, histidine decarboxylase knock-out mice, single-unit recording, sleep-waking discharge

INTRODUCTION

Histaminergic (HA) neurons in the tuberomammillary nucleus (TM) are the sole source of neuronal histamine in the mammalian brain and form widely branching neuronal pathways influencing large target fields, such as the norepinephrinergic (NE) neurons in the nucleus locus coeruleus (LC) and the serotonergic neurons in the dorsal raphe nucleus (DRN, Schwartz et al., 1991; Wada et al., 1991; Haas and Panula, 2003). The HA system is therefore thought to play an important role in a wide variety of physiological functions, including synaptic plasticity, learning, memory, energy and endocrine homeostasis, control of affective states, attention, and cognition (Haas and Panula, 2003; Haas et al., 2008). HA neurons play an important role in the forebrain waking systems (Wada et al., 1991; Monti, 1993; Lin, 2000). We previously reported that, in cats, presumed HA neurons exhibit tonic discharge that is highly waking (W)-specific (Sakai et al., 1990). In our recent study in mice, we found that HA neuronal activity is specific for a high vigilance W state and that HA neurons might play a role not in the initiation of W, but in the maintenance of the high level of vigilance necessary for cognitive processes (Takahashi et al., 2006). Accordingly, an increase in HA transmission promotes W, whereas its blockade causes somnolence and increased cortical slow activity (Schwartz et al., 1991; Monti, 1993; Lin, 2000; Yanai and Tashiro, 2007). Knock-out (KO) mice for histidine decarboxylase (HDC), the histamine-synthesizing enzyme, display a deficit of W and signs of somnolence when faced with a novel environment (Parmentier et al., 2002). HA neurons are therefore thought to promote W and cortical

activation through their widespread projections influencing many brain structures implicated in sleep-waking control (Lin, 2000; Haas and Panula, 2003; Anaclet et al., 2009).

Histaminergic neurons in the TM contain, in addition to histamine per se, other neurotransmitters and neuromodulators. The γ-aminobutyric acid (GABA)-synthesizing enzyme glutamic acid decarboxylase (GAD, Vincent et al., 1983; Takeda et al., 1984) and GABA itself are found in most TM neurons (Ericson et al., 1991; Airaksinen et al., 1992), as is adenosine deaminase (ADA), the enzyme catalyzing adenosine into inosine (Senba et al., 1985; Staines et al., 1986). An important question arises concerning the neuronal activity of TM neurons in HDC$^{-/-}$ mice. Do these TM "ex-HA neurons" (neurons that would normally contain histamine, but do not) display the same W-specific pattern of neuronal discharge as seen in wild-type (WT) HDC$^{+/+}$ mice? In order to answer this question, we first determined the activity of all neuron populations in the ventral tuberomammillary nucleus (VTM) of WT mice, then determined the characteristics of VTM neurons in HDC-KO mice.

MATERIALS AND METHODS
ANIMALS AND SURGERY

All procedures were approved by the University of Lyon 1 Animal Care Committee, the standards of which meet those of the EEC Guidelines (86/609/EEC) and the Policy on Ethics approved by the Society for Neuroscience (1993). All efforts were made to minimize the number of animals used and their suffering.

Fifteen adult male C57BL/6 WT mice (Harlan, France) and four adult male HDC-KO mice were used. The KO mice used in this study were from C57BL/6j strain, which was derived from backcrossing between male 129/Sv HDC-KO mice (Ohtsu et al., 2001) and female WT C57BL/6J mice for more than 15 generations. Our microsatellite analysis showed that the KO mice from this backcrossing have 0% 129/Sv background and between 99.9 and 100% C57BL/6J background, indicating that the WT and KO mice used in this study have the same genetic background except for HDC gene.

Their genotype with regard to the HDC gene was determined using the PCR protocol, as described previously (Anaclet et al., 2009). The mice were anesthetized using either pentobarbital (50 mg/kg, i.p.) or a mixture of 0.8 mg/ml ketamine and 1 mg/ml xylazine at an initial dose of 10 ml/kg, with 3 ml/kg boosters as needed, given i.p. The mice were placed in a stereotaxic apparatus (SN-3, Narishige, Tokyo, Japan) and implanted with electrodes to record the neocortical electroencephalogram (EEG), neck electromyogram (EMG), and electrocardiogram, as described previously (Takahashi et al., 2006). In addition, a U-shaped plastic plate (18 mm wide, 16 mm long, 5 mm thick) was fixed stereotaxically to the skull using dental acrylic cement so that the cranium could be painlessly returned to the same stereotaxic position using a semi-chronic head holder (Narishige, SA-8). After a recovery period of 1 week, the animals were habituated to the head-restrained position by placing them on a cotton sheet inside a plastic box, painlessly restraining the head with a semi-chronic head holder, and preventing large body movements with a cotton-coated plastic covering. The head was covered to reduce visual stimuli. After habituation, they could be kept in this position for three to five consecutive hours without showing any signs of discomfort and displayed complete sleep-waking cycles, consisting of W, slow-wave sleep (SWS), and paradoxical sleep (PS). If any signs of discomfort were seen, the mouse was freed from the restrained position.

EXTRACELLULAR SINGLE-UNIT AND POLYGRAPHIC RECORDINGS

Single neuronal activity was recorded extracellularly using a glass pipette microelectrode filled with 0.5 M sodium acetate containing 2% Pontamine Sky Blue, as previously described (Takahashi et al., 2006). Neuronal activity was amplified and filtered (NeuroLog, Digitimer, Hertfordshire, UK) with a cut off frequency of 100 Hz, then digitized at a sampling rate of 16.7–20.0 kHz using a CED 1410 data processor [Cambridge Electronic Design (CED), Cambridge, UK]. Polygraphic signals were also digitized at a sampling rate of either 504 or 512 Hz and stored on a personal computer. At the end of each experiment, Pontamine Sky Blue was injected from the recording electrode by passing a negative current (5 μA for 5–6 min) so as to mark one or two recording sites in each electrode track (see **Figure 2C**). Unit recordings were made during two experimental sessions per day and the experiments lasted five to six consecutive days. The animals were maintained on a 12 h light/dark schedule with lights on from 7 a.m. to 7 p.m., and recordings were usually made between 10 and 12 a.m. and between 2 and 5 p.m., periods in which mice normally sleep. They were fed with a standard normal diet [Ref. 801066 RM3 (E), Special Diets Services, Essex, England].

HISTOCHEMISTRY

At the end of the experiment, the animals were deeply anesthetized with pentobarbital, then perfused through the ascending aorta with 50 ml of Ringer's solution, followed by 150 ml of fixative consisting of 4% N-(3-dimethylaminopropyl)-carbodiimide (Sigma-Aldrich, GmbH, Germany) in 0.1 M phosphate buffer (PB), pH 7.4, followed by 100 ml of 4% paraformaldehyde. The brain was removed and postfixed for 48 h at 4°C in PB containing 4% N-(3-dimethylaminopropyl)-carbodiimide and 1% paraformaldehyde, then placed in PB containing 30% sucrose for 48 h at 4°C. Twenty micrometer sections were then cut on a cryostat and stored in 0.1 M phosphate-buffered saline containing 0.3% Triton X-100 (PBST) and 0.1% sodium azide until stained. Every third section was incubated for 4–8 days at 4°C with (1) rabbit anti-histamine antibodies (Millipore, Billerica, MA, USA), diluted 1/80,000, (2) mouse anti-GAD67 antibodies (Millipore, Billerica, MA, USA) diluted 1/10,000, or (3) rabbit anti-ADA antibodies (Millipore, Billerica, MA, USA) diluted 1/500, all in PBST containing 0.1% sodium azide. After several washes, the sections were incubated overnight at 4°C with biotinylated anti-rabbit or anti-mouse IgG antibodies (Vector Laboratories, Burlingame, CA, USA) diluted 1/1,000 in PBST, then, after several washes, were incubated for 90 min at room temperature with ABC (Vector Laboratories, diluted 1/1,000) and processed for visualization using DAB-nickel (Vector Laboratories) as chromogen. The sections were mounted on gelatin-coated glass slides, and processed with or without counterstaining with neutral red for observation under a light microscope.

DATA ANALYSIS

Sleep-waking stages were defined using the EEG and neck EMG signals. W was defined as low-voltage, desynchronized EEG or theta waves accompanying sustained EMG activity. The drowsy state (D) was defined as the first 3-s period from the onset of EEG synchronization during the transition from W to SWS, corresponding to the beginning of light SWS. SWS was defined either by slow EEG waves with variable amplitude and frequency and lowered EMG activity (light SWS or S1) or by sustained high-voltage and low frequency waves in the EEG and lowered EMG activity (deep SWS or S2). PS was defined by sustained theta waves and decreased delta waves in the EEG and the absence of EMG activity. Power spectra were computed for 1-s epochs using a Fast Fourier Transform routine and the Spike2 analysis program (CED), which was also used for the analysis of unitary activity. Mean discharge rates were calculated from total recordings using 2–10 s bins for each of the following states: (1) attentive or active waking (AW), characterized by either overt body and limb movements and by a low amplitude (desynchronized) EEG with a sustained EMG activity (2- to 5-s bin); (2) quiet waking (QW), characterized by the absence of gross movements (3- to 10-s bin); (3) D (3-s bin); (4) SWS (S2, 10-s bin); and (5) PS (10-s bin). Statistical analysis was carried out using the Kruskal–Wallis test and *post hoc* Mann–Whitney test, a *P*-value of <0.05 or <0.01 being considered, respectively, as significant or highly significant.

RESULTS

HA AND "ex-HA" NEURONS IN THE TM

As in the rat brain (Ericson et al., 1987), we found that the mouse TM could be subdivided into medial (MTM), ventral (VTM), and diffuse (DTM) subgroups using histamine

immunohistochemistry (**Figures 1A–C**), with the VTM containing the densest population of HA neurons. **Figure 2B** shows a photomicrograph of a section, which shows the VTM neurons in a WT (HDC⁺/⁺) mice, immunostained for HA neurons (black labeling) and counterstained with neutral red to show non-HA neurons (red color alone). As seen in this photomicrograph, many VTM neurons were immunoreactive for histamine, but a significant number of non-HA neurons were also found within the VTM. HDC-KO mice, confirmed by the PCR method (**Figure 2A**), showed no histamine-positive VTM neurons (**Figure 2C**). However, the magnocellular VTM neurons were clearly visualized in HDC-KO mice using Nissl-staining (**Figure 2C**) and immunostaining with either anti-ADA (**Figure 2D**) or anti-GAD67 (**Figure 2E**) antibodies, thus proving the "ex-HA neuron" identity of these VTM neurons.
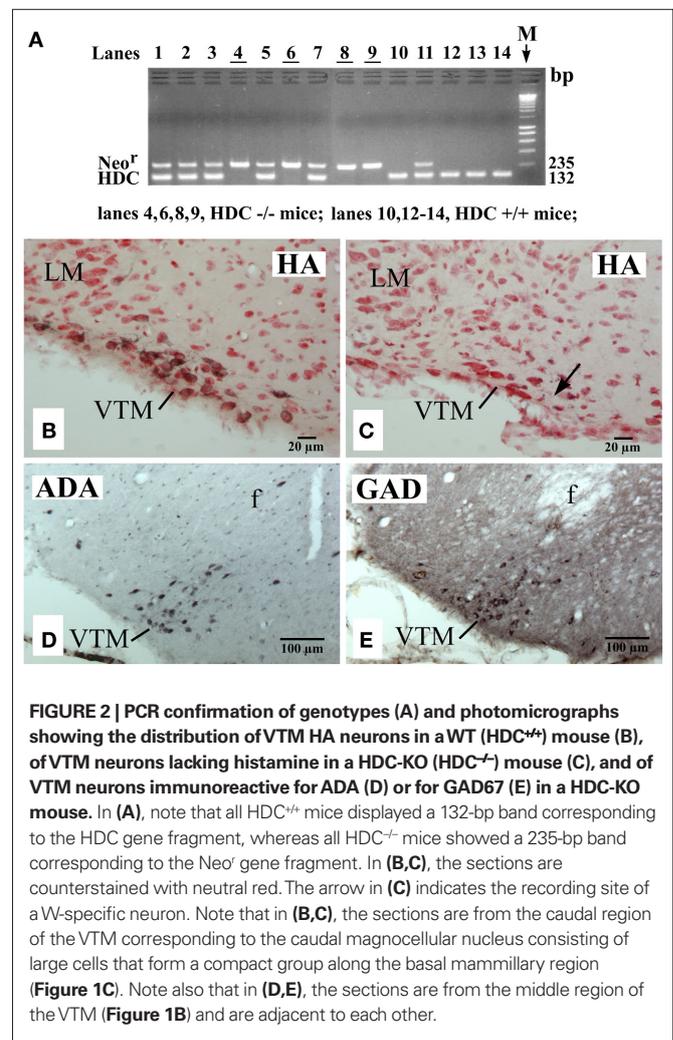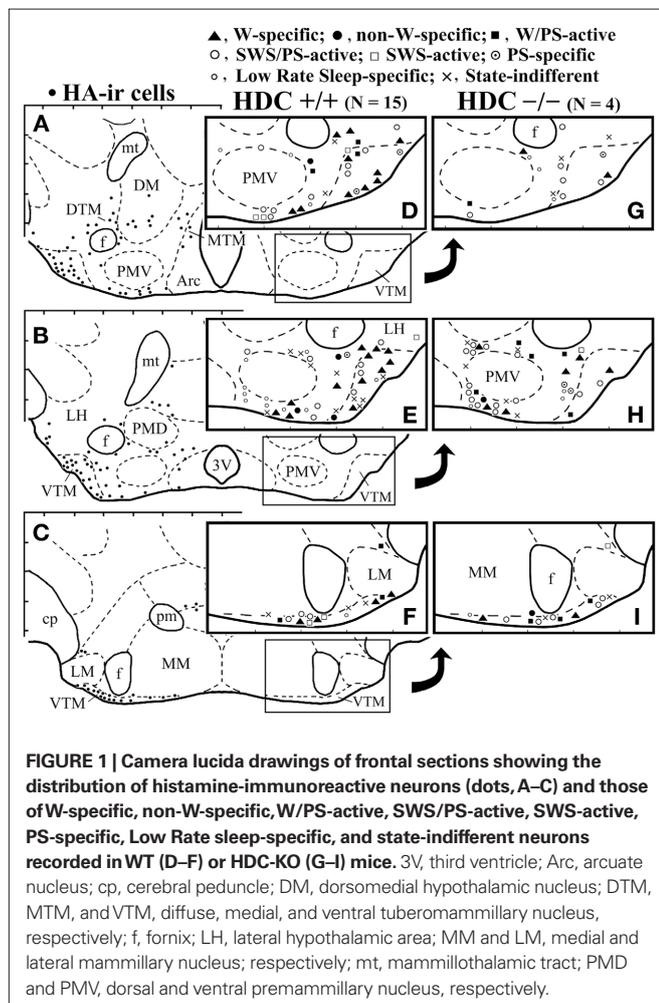
DIFFERENT GROUPS OF VTM NEURONS IN WT MICE

A total of 92 single units were recorded in the ventrolateral region of the posterior hypothalamus (PH) containing HA neurons, in particular the VTM (**Figures 1D–F**) of 15 WT mice. On the basis of differences in their firing patterns and rates during the sleep-waking cycle (**Table 1**), one group of state-unrelated ($n = 13$; 14.1%)

and three groups of state-related neurons were identified, the latter being W-active ($n = 30$; 32.6%), W/PS-active ($n = 6$; 6.5%), and sleep-active ($n = 43$; 46.7%).
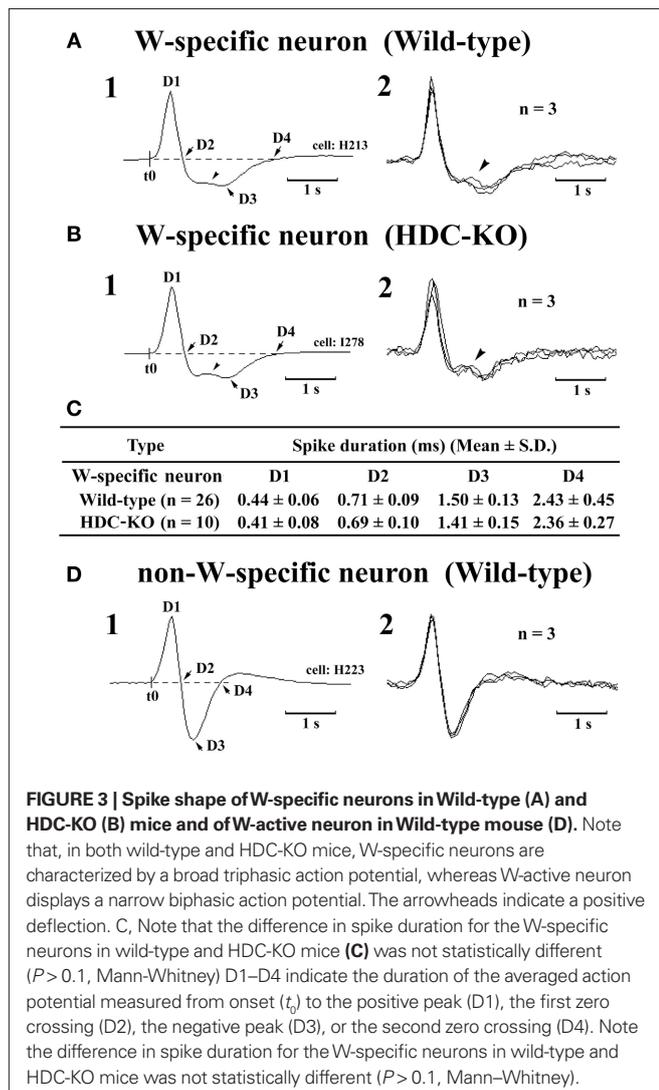
W-active neurons

The W-active neurons were divided into W-specific ($n = 26$) and non-W-specific ($n = 4$) subgroups (**Table 1**). The W-specific neurons had a broad triphasic action potential (**Figure 3A**) and discharged only during W, whereas non-W-specific neurons had a narrow biphasic action potential (**Figure 3D**) and showed reduced, but persistent, discharge during SWS and PS (**Table 1**). The mean (±SD) spike duration (positive inflection to first zero crossing (D2; see **Figure 3**) for the W-specific or non-W-specific neurons was 0.71 ± 0.09 or 0.62 ± 0.62 ms, respectively. Our previous study in mice (Takahashi et al., 2006) demonstrated that these W-specific and non-W-specific neurons are, respectively, HA and non-HA neurons. Changes in unit activity during the transitions from SWS to W and from W to SWS were examined using 0.1-s bins for five VTM W-specific neurons showing many state transitions. As shown in **Figure 4** (upper panel), during the transition from SWS to W, the W-specific neurons began to fire after the onset of W,

FIGURE 1 | Camera lucida drawings of frontal sections showing the distribution of histamine-immunoreactive neurons (dots, A–C) and those of W-specific, non-W-specific, W/PS-active, SWS/PS-active, SWS-active, PS-specific, Low Rate sleep-specific, and state-indifferent neurons recorded in WT (D–F) or HDC-KO (G–I) mice. 3V, third ventricle; Arc, arcuate nucleus; cp, cerebral peduncle; DM, dorsomedial hypothalamic nucleus; DTM, MTM, and VTM, diffuse, medial, and ventral tuberomammillary nucleus, respectively; f, fornix; LH, lateral hypothalamic area; MM and LM, medial and lateral mammillary nucleus; respectively; mt, mammillothalamic tract; PMD and PMV, dorsal and ventral premammillary nucleus, respectively.

FIGURE 2 | PCR confirmation of genotypes (A) and photomicrographs showing the distribution of VTM HA neurons in a WT (HDC⁺/⁺) mouse (B), of VTM neurons lacking histamine in a HDC-KO (HDC⁻/⁻) mouse (C), and of VTM neurons immunoreactive for ADA (D) or for GAD67 (E) in a HDC-KO mouse. In (A), note that all HDC⁺/⁺ mice displayed a 132-bp band corresponding to the HDC gene fragment, whereas all HDC⁻/⁻ mice showed a 235-bp band corresponding to the Neoʳ gene fragment. In (B,C), the sections are counterstained with neutral red. The arrow in (C) indicates the recording site of a W-specific neuron. Note that in (B,C), the sections are from the caudal region of the VTM corresponding to the caudal magnocellular nucleus consisting of large cells that form a compact group along the basal mammillary region (Figure 1C). Note also that in (D,E), the sections are from the middle region of the VTM (Figure 1B) and are adjacent to each other.

Table 1 | Cell counts and mean discharge rates during the sleep-waking cycle of state-dependent and state-unrelated ventral tuberomammillary neurons in wild-type mice.

	Cell type	Number (percentage) of recorded neurons	Mean discharge rate (±SEM)						
			AW	QW	D	SWS	PS	*H*	*P*
1	W-active	30 (32.6%)							
	a. W-specific	26 (28.3%)	4.24 ± 0.28	3.09 ± 0.24	0.00 ± 0.00	0.00 ± 0.00	0.00 ± 0.00	119.2	<0.0001
	b. non-W-specific	4 (4.3%)	8.57 ± 2.73	4.77 ± 1.48	0.97 ± 0.10	0.40 ± 0.25	0.80 ± 0.25	14.1	<0.01
2	W/PS-active	6 (6.5%)	2.74 ± 0.64	2.12 ± 0.49	0.58 ± 0.27	0.82 ± 0.27	3.08 ± 0.91	13.3	<0.01
3	Sleep-active	43 (46.7%)							
	a. SWS-active	6 (6.5%)	0.34 ± 0.19	0.37 ± 0.19	3.83 ± 1.31	9.94 ± 2.74	4.96 ± 2.08	20.1	<0.001
	b. SWS/PS-active	20 (21.7%)	0.23 ± 0.09	0.35 ± 0.12	1.82 ± 0.44	3.07 ± 0.72	4.09 ± 0.61	59.7	<0.0001
	c. PS-specific	3 (3.3%)	0.01 ± 0.01	0.00 ± 0.00	0.05 ± 0.05	0.55 ± 0.27	4.23 ± 1.56	12.3	<0.01
	d. Low rate (<1 Hz)	14 (15.2%)	0.00 ± 0.00	0.01 ± 0.01	0.09 ± 0.05	0.36 ± 0.08	0.55 ± 0.07	52.1	<0.0001
4	Unrelated	13 (14.1%)	5.98 ± 2.08	4.91 ± 1.59	4.30 ± 1.36	4.77 ± 1.34	5.09 ± 2.17	0.83	0.93
	Total	92							

Statistical analysis was carried out using the Kruskal–Wallis test.

FIGURE 3 | Spike shape of W-specific neurons in Wild-type (A) and HDC-KO (B) mice and of W-active neuron in Wild-type mouse (D). Note that, in both wild-type and HDC-KO mice, W-specific neurons are characterized by a broad triphasic action potential, whereas W-active neuron displays a narrow biphasic action potential. The arrowheads indicate a positive deflection. C, Note that the difference in spike duration for the W-specific neurons in wild-type and HDC-KO mice **(C)** was not statistically different ($P > 0.1$, Mann-Whitney) D1–D4 indicate the duration of the averaged action potential measured from onset (t_0) to the positive peak (D1), the first zero crossing (D2), the negative peak (D3), or the second zero crossing (D4). Note the difference in spike duration for the W-specific neurons in wild-type and HDC-KO mice was not statistically different ($P > 0.1$, Mann–Whitney).

defined by the onset of EEG activation. The mean (±SEM) latency for all W-specific neurons was 859.7 ± 88.0 ms. During the transition from W to SWS (**Figure 4**, lower panel), they ceased firing before the onset of EEG synchronization (deactivation), the first sign of SWS (drowsy state, D). The mean (±SEM) interval between the last spike discharge and the onset of D was 953.9 ± 55.0 ms ($n = 26$). As shown in **Figure 4** (lower panel), they showed a significant decrease in firing rate as early as 1 s before the onset of D, as previously described for HA TM neurons in general (Takahashi et al., 2006, 2009).

W/PS-active neurons

This minor group of neurons ($n = 6$; 6.5%) had a bipolar action potential with a mean (±SD) spike duration (D2) of 0.60 ± 0.13 ms, significantly shorter than that of the W-specific neurons ($P < 0.05$, Mann–Whitney). They displayed a slow tonic discharge, their mean spontaneous firing rate being significantly higher during W and PS than during SWS (**Table 1**; $P < 0.05$, Mann–Whitney). However, there was no statistically significant difference in firing rate between AW and QW and between W and PS ($P > 0.05$, Mann–Whitney).

Sleep-active neurons

Sleep-active neurons represented 46.7% of the total neurons and were divided into the four subgroups of SWS-active ($n = 6$), SWS/PS-active ($n = 20$), PS-specific ($n = 3$), and Low Rate ($n = 14$) (**Table 1**).

SWS-active neurons. They had a higher rate of spontaneous discharge during SWS than during W and PS; 3 were completely silent during both AW and W and will be referred to hereafter as SWS-specific neurons (**Figure 5**). The overall SWS-active neurons had a biphasic action potential and a mean (±SD) spike duration (D2) of 0.60 ± 0.09 ms, significantly shorter than that of the W-specific neurons ($P < 0.05$, Mann–Whitney). Although the SWS-active neurons displayed a higher rate of discharge during SWS than during D, the difference was not statistically different ($P > 0.05$,
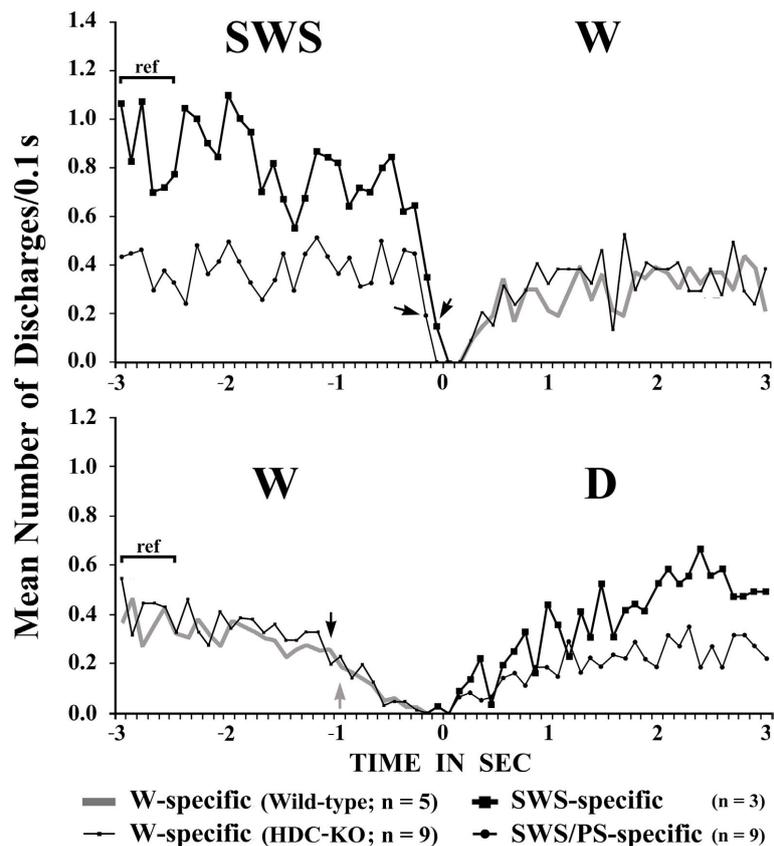
FIGURE 4 | Mean time-course of the discharge rate for VTM W-specific neurons recorded in wild-type or HDC-KO mice and for VTM SWS-specific and SWS/PS-specific neurons in wild-type mice at the transition from SWS to W (upper panel) and from waking to D (lower panel). Each group is represented by the symbol indicated on the figure. The pooled mean frequency using 0.1-s bins was obtained from more than 40 transitions observed in 3, 5, or 9 neurons from each WT VTM 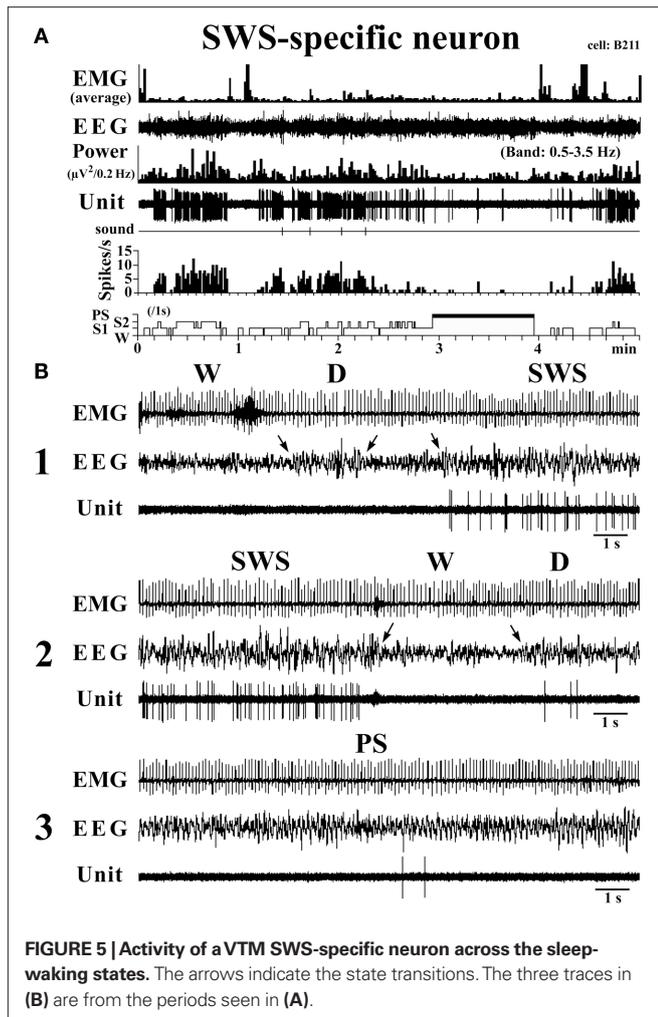neuron group and in 9 HDC-KO W-specific neurons. 0 indicates the onset of EEG activation in the upper panel and the onset of EEG synchronization (deactivation) in the lower panel. The statistical significance of the difference between the discharge rate going from SWS to W (upper panel) or from W to drowsy state (lower panel) and the reference discharge rate seen during the 0.6-s period of SWS or W from 3 to 2.4 s before the onset of the state transition was examined. The arrows indicate the first point at which a statistically significant decrease in firing rate was observed (Mann–Whitney).

Mann–Whitney). The activity profiles for the SWS-specific neurons during wake–sleep state transitions were examined using 0.1-s bins and are shown in **Figure 4**. The SWS-specific neurons ceased firing just before the onset of EEG activation during the transition from SWS to W (**Figure 4**, upper panel, and **Figure 5B-2**) and discharged, except one case, after the onset of EEG activation during the transition from W to D (**Figure 4**, lower panel, and **Figure 5B-1**).

SWS/PS-active neurons. These had a higher rate of spontaneous discharge during SWS and PS than during W, the discharge rate during PS being higher than during SWS and statistically different ($P < 0.05$, Mann–Whitney). They had a bipolar action potential with a duration (D2) of 0.60 ± 0.09 ms, statistically different from that of the W-specific neurons ($P < 0.05$; Mann–Whitney). Sixteen of the 20 SWS/PS-active neurons displayed no discharge during W and are referred to hereafter as SWS/PS-specific neurons (**Figure 6**). As shown in **Figure 6**, the SWS/PS-specific neurons ceased firing prior to the onset of EEG activation during the transition from SWS to W either occurring spontaneously or elicited by an arousing sound stimulus (**Figure 6B-2**). During the transition

from W to D, they fired after the onset of EEG synchronization (deactivation) (**Figure 6B-3**), 7 of the 16 displaying no discharge during the 3-s period of D. The time-course of the unit discharge during the state transitions was then estimated in the remaining nine SWS/PS-specific neurons. **Figure 4** shows that, like the SWS-specific neurons, the SWS/PS-specific neurons ceased firing just before the onset of discharge of the W-specific neurons during the transition from SWS to W, while, during the transition from W to D, they discharged after cessation of discharge of the W-specific neurons.

PS-specific neurons. Three neurons showed no discharge during W and exhibited a slow tonic discharge that was highly specific for PS, the spontaneous firing rate during PS being at least five times as high as that during SWS. They had a broad bipolar action potential with a mean ($\pm$SD) spike duration of 0.73 ± 0.06 ms, not statistically different from that of W-specific neurons ($P > 0.05$, Mann–Whitney). During the transition from PS to W, they ceased firing before the end of rhythmic theta waves, with a mean ($\pm$SEM) interval of 520.3 ± 374.8 ms.
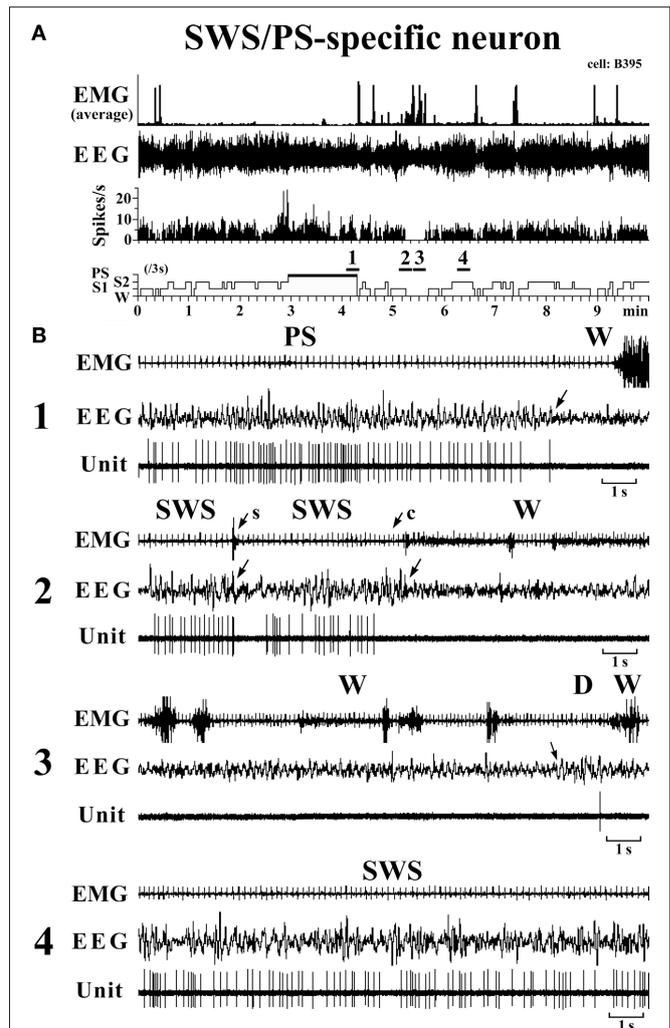
FIGURE 5 | Activity of a VTM SWS-specific neuron across the sleep-waking states. The arrows indicate the state transitions. The three traces in **(B)** are from the periods seen in **(A)**.

FIGURE 6 | Activity of a VTM SWS/PS-specific neuron across the sleep-waking states. The arrows indicate the state transitions. The arrows with "s" or "c" indicate W elicited by an sound stimulus or removing the cover placed over the head of the mouse, respectively. The four traces in **(B)** are from the periods indicated by the bar under, respectively, "1", "2", "3", and "4" in **(A)**.

Low Rate sleep-specific neurons. Fourteen of the 92 neurons were characterized by a very low unit activity (<1.0 Hz) that was specific for SWS and PS. The vast majority (12/14) had a biphasic narrow action potential and an overall spike duration (D2) of 0.59 ± 0.11 ms, statistically different from that of the W-specific neurons ($P < 0.01$, Mann–Whitney). They were mostly located around the ventral premammillary nucleus (PMV, **Figures 1D–F**).

State-indifferent neurons. Thirteen of the 92 neurons (14.1%) showed state-indifferent unit activity. They had a biphasic action potential with a mean ($\pm$SD) spike duration of 0.60 ± 0.08 ms, statistically different from that of the W-specific neurons ($P < 0.001$, Mann–Whitney).

TM NEURONS IN HD-KO MICE
A total of 69 single units were recorded in the ventrolateral region of the PH of 4 HDC-KO mice (**Figures 1G–I**). As in WT mice, four groups of neurons were identified: W-active ($n = 12$; 17.4%), W/PS-active ($n = 9$; 13.0%), sleep-active ($n = 36$; 52.2%), and state-unrelated ($n = 11$; 15.9%) (**Table 2**). The W-active neurons were composed of W-specific ($n = 10$) and non-W-specific ($n = 2$) neurons and the sleep-active neurons were composed of SWS-active ($n = 2$), SWS/PS-active ($n = 25$), PS-specific ($n = 3$), and Low Rate

($n = 7$) neurons; their mean spontaneous discharge rates are presented in **Table 2**. Since the characteristics of the state-dependent and state-unrelated neurons in the HDC-KO mice were very similar to those in the WT mice, they will not be described further. Instead, we will describe in detail the characteristics of the W-specific neurons in the HDC-KO mice and compare them with those in WT mice. **Figure 2C** shows the recording site (indicated by an arrow) in a W-specific neuron in the VTM of an HDC-KO mouse.

W-specific neurons in HDC-KO mice
The W-specific neurons in HDC-KO mice were all characterized by having a broad triphasic action potential (**Figure 3B**), with mean durations (D1–D4) not significantly different from those in W-specific neurons in WT mice ($P > 0.1$, Mann–Whitney) (**Figure 3C**). As shown in **Figure 7**, they displayed a slow tonic discharge that was specific for waking states. They fired at higher rates during AW than during QW,

Table 2 | Cell counts and mean discharge rates during the sleep-waking cycle of state-dependent and state-unrelated ventral tuberomammillary neurons in histidine decarboxylase knock-out mice.

	Cell type	Number (percentage) of recorded neurons	Mean discharge rate (±SEM)						
			AW	QW	D	SWS	PS	*H*	*P*
1	W-active	12 (17.4%)							
	a. W-specific	10 (14.5%)	4.04 ± 0.39	3.04 ± 0.42	0.00 ± 0.00	0.00 ± 0.00	0.00 ± 0.00	40.8	<0.0001
	b. non-W-specific	2 (2.9%)	6.72 ± 0.61	6.67 ± 1.42	1.74 ± 1.41	0.28 ± 0.28	1.83 ± 0.52	–	–
2	W/PS-active	9 (13.0%)	6.27 ± 0.94	5.15 ± 0.77	1.38 ± 0.50	1.44 ± 0.84	4.23 ± 1.37	19.4	<0.001
3	Sleep-active	36 (52.2%)							
	a. SWS-active	2 (2.9%)	5.54 ± 3.79	6.37 ± 3.22	10.84 ± 5.95	14.66 ± 7.62	8.53 ± 6.88	–	–
	b. SWS/PS-active	25 (36.2%)	0.92 ± 0.37	0.82 ± 0.31	1.58 ± 0.40	2.94 ± 0.58	5.29 ± 1.01	52.7	<0.00010
	c. PS-specific	3 (4.3%)	0.00 ± 0.00	0.00 ± 0.00	0.00 ± 0.00	0.62 ± 0.38	3.71 ± 1.96	13.4	<0.01
	d. Low rate (<1 Hz)	7 (10.1%)	0.02 ± 0.02	0.03 ± 0.03	0.15 ± 0.11	0.46 ± 0.11	0.78 ± 0.07	24.2	<0.0001
4	Unrelated	11 (15.9%)	14.06 ± 7.34	8.46 ± 3.46	8.88 ± 4.03	8.03 ± 3.13	8.96 ± 3.03	0.99	0.91
	Total	69							

Statistical analysis was carried out using the Kruskal–Wallis test.

but the difference was not statistically significant ($P > 0.05$, Mann–Whitney). When the mice entered a steady sleep state, the brief interruptions of sleep caused by body movements were not accompanied by any spike discharge (**Figure 7A**, arrow on the hypnogram). The mean (±SEM) spontaneous discharge rates of W-specific neurons in HDC-KO mice during AW (4.04 ± 0.39) and QW (3.04 ± 0.42) were not statistically different from those (4.24 ± 0.28 and 3.09 ± 0.24 ms, respectively) in WT mice ($P > 0.05$, Mann–Whitney). During the spontaneous transition from SWS to W (**Figure 7B-4**), the W-specific neurons in KO mice fired after the onset of EEG activation, with a mean (±SEM) latency of 679.26 ± 95.42 ms, not significantly different from that seen in WT mice (859.73 ± 87.95 ms) ($P > 0.05$, Mann–Whitney). When waking was elicited by an arousing sound stimulus (**Figure 7B-2**), the W-specific neurons in the HDC-KO mice either responded to the stimulus with a pronounced delay (mean minimal latency ± SEM, 428.81 ± 92.67 ms) or did not respond at all (latency >2 s), as seen with the W-specific neurons in WT mice. During the transition from W to SWS, they stopped firing before the onset of EEG synchronization (deactivation), with a mean (±SEM) latency of 743.17 ± 82.03 ms, not statistically different from that seen in WT mice (953.85 ± 54.94 ms) ($P > 0.05$, Mann–Whitney). Finally, during the transition from PS to W, they discharged after the end of PS, defined by the end of continuous rhythmic theta waves, with a mean (±SEM) interval of 1577.60 ± 29.48 ms, not statistically different from that seen in WT mice (3562.29 ± 1256.89 ms) ($P > 0.05$, Mann–Whitney). The mean time-course of the unit discharge at the transitions from SWS to W and from W to D for the W-specific neurons in HDC-KO mice was estimated using 0.1-s bins. As seen in **Figure 4**, their time-course closely overlapped with that of WT mice at the transitions from SWS to W (upper panel) and from W to D (lower panel).

DISCUSSION

WAKING-SPECIFIC NEURONS IN HDC-KO MICE ARE ex-HA NEURONS

In the present study on the VTM in WT mice, we identified three groups of state-dependent and one group of state-indifferent neurons and determined their characteristics in terms of spike shape and discharge property across the sleep-waking cycle. In the VTM in HDC-KO mice, we found exactly the same groups of neurons, including W-specific ones. Using extracellular single-unit recordings in combination with neurobiotin juxtacellular labeling and histamine immunohistochemistry, we have previously demonstrated that W-specific neurons and other types of neurons in the TM of WT mice are, respectively, histaminergic and non-histaminergic (Takahashi et al., 2006). The W-specific neurons in HDC-KO mice were located in the VTM region, where W-specific HA neurons were found in WT mice (**Figure 1**, see also Takahashi et al., 2006). The VTM in HDC-KO mice contained no histamine-immunoreactive neurons, but was characterized by the presence, as in WT mice, of Nissl-stained magnocellular neurons and neurons immunoreactive for ADA and GAD67, markers for HA neurons other than histamine itself (**Figure 2**). The VTM W-specific neurons in HDC-KO mice displayed a broad triphasic action potential (**Figure 3**) and their unit activity was high vigilance W-specific (**Figure 7**). They either responded to an arousing sound stimulus with a pronounced delay or did not respond at all when the stimulus did not elicit the steady state of alertness marked by sustained EEG desynchronization or theta waves. During the transition from waking to sleep, they stopped firing before the onset of EEG synchronization, the first sign of EEG sleep, while, during the transition from sleep to waking, they discharged not before, but after, onset of EEG activation, the first sign of EEG waking (**Figure 4**). The VTM W-specific neurons in HDC-KO mice thus displayed exactly the same characteristics as those in WT mice. These findings strongly suggest that the VTM W-specific neurons in HDC-KO mice are ex-HA neurons, and that these ex-HA neurons exhibit W-specific neuronal activity even in the absence of endogenous histamine. At present, it is not known whether these ex-HA neurons exhibit *in vitro* the same basic electrophysiological properties as those of WT mice. However, it is worth mentioning that, in brain slices from dopamine β-hydroxylase KO mice, which lack norepinephrine, neurons in the substantia nigra pars compacta and LC display the same spontaneous firing and pattern as seen in control mice (Paladini et al., 2007). It is known

FIGURE 7 | Activity of a VTM W-specific neuron recorded in a HDC-KO mouse. The unlabeled arrows indicate the state transitions, while the arrows with "s" or "t" indicate W elicited by an sound stimulus or touching the tail with a soft brush. The four traces in **(B)** are from the periods indicated by the bar under, respectively, "1", "2", "3" and "4" in **(A)**.

that the morphological and electrophysiological properties of HA neurons are similar to those seen in other aminergic neuron populations (see Haas et al., 2008). It therefore appears that, in the same way that endogenous norepinephrine is not essential for the firing of NE neurons, endogenous histamine is not necessary for the expression of the firing properties of HA neurons. Finally, in the present study, the neurochemical identity of the W-specific neurons was not determined using neurobiotin juxtacellular labeling and subsequent ADA/GAD immunohistochemistry, and this should be done in further studies.

FUNCTIONAL ROLE OF ex-HA NEURONS IN THE CONTROL OF VIGILANCE

HA neurons in the TM receive both excitatory and inhibitory inputs. The inhibitory inputs come from neurons with an inhibitory amino acid transmitter, GABA, while the excitatory inputs come from neurons with an excitatory amino acid transmitter,

glutamate, and the excitatory neuropeptides orexin/hypocretin (Orx/Hcrt, Brown et al., 2001; Haas et al., 2008). The fact that the VTM ex-HA neurons displayed the same firing properties as VTM HA neurons throughout the sleep-waking cycle leads us to suppose that the ex-HA neurons have the same neuronal connectivity as the VTM HA neurons in WT mice. The maintenance of such synaptic connectivity may play a role in the maintenance of the membrane and neuron firing properties of the VTM ex-HA neurons. Both Orx/Hcrt and possibly glutamatergic non-Orx/Hcrt neurons in the PH in mice display W-specific neuronal activity (Takahashi et al., 2008). Inhibitory GABAergic inputs to TM HA neurons come from several preoptic/basal forebrain (POA/BFB) and lateral hypothalamic structures, in particular the ventrolateral preoptic area which contains sleep-active neurons and is thereby thought to play a role in the suppression of activity of TM HA neurons during sleep (reviewed in Jones, 2005; Saper et al., 2005; Szymusiak et al., 2007; Haas et al., 2008). In the present study, we discovered many sleep-active neurons in the VTM of both WT and HDC-KO mice, including SWS-specific and SWS/PS-specific neurons, the activity of which was opposed to that of W-specific neurons at the transitions from SWS to W and from W to D (**Figure 4**). It seems likely that these VTM sleep-specific neurons play an important role in the control of the activity of TM HA neurons in general. At the transition from W to SWS, the VTM sleep-specific neurons discharged, not before, but after cessation of activity of the VTM W-specific neurons, as seen with the SWS-specific and SWS/PS-specific neurons in the POA/BFB of WT mice (Takahashi et al., 2009), a fact that refutes the general hypothesis that cessation of activity of TM HA neurons results from the activation of sleep-active neurons (reviewed in Jones, 2005; Saper et al., 2005; Szymusiak et al., 2007). On the other hand, at the transition from SWS to W, all the VTM W-specific neurons discharged after the cessation of discharge of sleep-specific neurons in the POA/BFB (Takahashi et al., 2009) and VTM (the present study; **Figure 4**, upper panel), in line with the hypothesis that the activation of HA W-specific neurons at W onset is due to the cessation of activity of the sleep-specific neurons using GABA as their main neurotransmitter. Unlike the VTM W-specific neurons, our recent studies in WT mice showed that, at the transition from SWS to W, W-specific neurons in the POA/BFB and Orx–Hcrt and non-Orx–Hcrt waking-specific neurons in the PH discharge before the onset of cortical activation and the start of a significant decrease in activity of sleep-specific neurons in the POA/BFB (Takahashi et al., 2008, 2009), as seen with W-specific NE–LC neurons in WT mice (Takahashi et al., 2010). The interval between the first unit discharge and the onset of EEG activation in these W-specific neurons decreased in the order NE–LC > POA/BFB > Orx–Hcrt = non-Orx–Hcrt (Takahashi et al., 2010), suggesting that these waking-specific neurons constitute important waking-promoting neural elements, playing a role in both the induction and maintenance of W. These results further suggest that the waking process starts with the excitation of NE–LC neurons, which leads to a cascade of excitation of waking-promoting neurons and inhibition of sleep-promoting neurons, thereby reinforcing the waking process.

Neuronal histamine, stored in axon varicosities, is released on arrival of action potentials (Haas et al., 2008). Three histamine receptors, H_1, H_2, and H_3, have been identified in the brain. The H_1

and H_2 receptors mainly mediate excitatory postsynaptic actions, whereas H_3 receptors, located on histaminergic and other cell somata, dendrites, and axons, cause autoinhibition of TM HA neurons and inhibition of the release of other neurotransmitters (Schwartz et al., 1991; Haas and Panula, 2003; Haas et al., 2008). Histamine exerts excitatory effects on whole brain activity through H_1 receptors, while the blockade of H_1 receptors by H_1 receptor antagonists, commonly known as anti-histamines, evokes sedation in humans (Schwartz et al., 1991; Yanai and Tashiro, 2007). Local injection of muscimol, a potent $GABA_A$ receptor agonist, into the VTM region causes hypersomnia in several species and restores sleep in various insomniac models in the cat (Lin, 2000). Histamine has excitatory actions on thalamic relay neurons (McCormick and Williamson, 1989, 1991), cholinergic neurons of the brainstem and basal forebrain (Khateb et al., 1995; Lin et al., 1996; Crochet and Sakai, 1999; Koyama and Sakai, 2000), and serotonergic neurons of the DRN (Sakai and Crochet, 2000; Brown et al., 2002), all implicated in waking and attention. Recent studies have demonstrated that HDC-KO mice display a deficit of waking and signs of somnolence when faced with a novel environment (Parmentier et al., 2002).

Tuberomammillary Nucleus HA neurons synthesize and release GABA, a potent and well-known inhibitory neurotransmitter. Indeed, most HA neurons contain the GABA-synthesizing enzyme GAD and GABA itself (see Haas and Panula, 2003 for review). The first paper that reported the GABAergic nature of TM neurons (Vincent et al., 1983) appeared even before their identification as HA neurons (Panula et al., 1984; Takeda et al., 1984; Watanabe et al., 1984). What is the function in behavioral state control of GABA, which might be the main neurotransmitter in HDC-KO mice? Early electron microscopic observations revealed that only 3 of 25 serially cut HDC-immunoreactive axonal varicosities formed synaptic contacts (Hayashi et al., 1984), leading to the postulate that the majority of HA axons release histamine non-synaptically and that this non-synaptically released histamine affects neurons in the vicinity in the same way as neurohormones or neuromodulators (Hayashi et al., 1984; Wada et al., 1991), as seen with other biogenic amines (Beaudet and Descarries, 1978). At present, it is unclear whether HA axons release GABA both synaptically and non-synaptically and affect both synaptic and extrasynaptic GABA receptors, thereby having a significant inhibitory effect on target neurons. Although no information is available about the postsynaptic mechanisms (transmitter release and contact formation) of ex-HA neurons, if GABA were released from the axon varicosities of these ex-HA neurons, it might exert a significant physiological impact on their target neurons implicated in the control of behavioral states. The deficit in vigilance seen in HDC-KO mice might be due, at least in part, to the action of GABA released from ex-HA neurons, the inhibitory action of which is opposed to the normal excitatory actions of histamine release. When specifically activated during waking, W-specific ex-HA neurons, which probably have the same widespread projection system as HA neurons, could mediate general inhibition throughout the brain and thus exert a significant influence on a variety of physiological functions. Further studies are needed to determine the exact role of the W-specific ex-HA neurons which may use GABA as their main neurotransmitter. Finally, it should be mentioned that, in addition to GABA, several neuropeptides, such as galanin, enkephalin, thyrotropin-releasing hormone, proenkephalin-derived peptides, and substance P, are also found in some histamine-containing TM neurons. It seems likely that these cotransmitters have inhibitory or excitatory effects on sleep-promoting and/or waking-promoting neurons. Although presumed GABAergic sleep-promoting neurons in the VLPO have been reported to be unaffected by histamine (Gallopin et al., 2000, but see Liu et al., 2010), some of these cotransmitters might have inhibitory or excitatory actions on these sleep-promoting neurons.

CONCLUSIONS

The present study strongly suggests that the ventral tuberomammillary waking-specific neurons in HDC-KO are ex-histaminergic neurons and that endogenous histamine is not necessary for the expression of histaminergic neuron firing properties.

ACKNOWLEDGMENTS

REFERENCES

Airaksinen, M. S., Alanen, S., Szabat, E., Visser, T. J., and Panula, P. (1992). Multiple neurotransmitters in the tuberomammillary nucleus: comparison of rat, mouse, and guinea pig. *J. Comp. Neurol.* 323, 103–116.

Anaclet, C., Parmentier, R., Ouk, K., Guidon, G., Buda, C., Sastre, J. P., Akaoka, H., Sergeeva, O. A., Yanagisawa, M., Ohtsu, H., Franco, P., Haas, H. L., and Lin, J. S. (2009). Orexin/hypocretin and histamine: distinct roles in the control of wakefulness demonstrated using knock-out mouse models. *J. Neurosci.* 29, 14423–14438.

Beaudet, A., and Descarries, L. (1978). The monoamine innervation of rat cerebral cortex: synaptic and non-synaptic axon terminals. *Neuroscience* 3, 851–860.

Brown, R. E., Sergeeva, O. A., Eriksson, K. S., and Haas, H. L. (2002). Convergent excitation of dorsal raphe serotonin neurons by multiple arousal systems (orexin/hypocretin, histamine and noradrenaline). *J. Neurosci.* 22, 8850–8859.

Brown, R. E., Stevens, D. R., and Haas, H. L. (2001). The physiology of brain histamine. *Prog. Neurobiol.* 63, 637–672.

Crochet, S., and Sakai, K. (1999). Effects of microdialysis application of monoamines on the EEG and behavioural states in the cat mesopontine tegmentum. *Eur. J. Neurosci.* 11, 3738–3752.

Ericson, H., Köhler, C., and Blomqvist, A. (1991). GABA-like immunoreactivity in tuberomammillary nucleus: an electron microscopic study in the rat. *J. Comp. Neurol.* 305, 462–469.

Ericson, H., Watanabe, J., and Köhler, C. H. (1987). Morphological analysis of the tuberomammillary nucleus in the rat brain: delineation of subgroups with antibody against L-histidine decarboxylase as a marker. *J. Comp. Neurol.* 263, 1–24.

Gallopin, T., Fort, P., Eggermann, E., Cauli, B., Luppi, P.H., Rossier, J., Audinat, E., Mühlethaler, M., Serafin, M. (2000). Identification of sleep-promoting neurons in vitro. *Nature* 404, 992–995.

Haas, L. H., and Panula, P. (2003). The role of histamine and the tuberomamillary nucleus in the nervous system. *Nat. Rev. Neurosci.* 4, 121–130.

Haas, L. H., Sergeeva, O. A., and Selbach, O. (2008). Histamine in the nervous system. *Physiol. Rev.* 88, 1183–1241.

Hayashi, H., Takagi, H., Takeda, N., Kubota, Y., Tohyama, M., Watanabe, T., and Wada, H. (1984). Fine structure of histaminergic neurons in the caudal magnocellular nucleus of the rat as demonstrated by immunohisto-

chemistry using histidine decarboxylase as a marker. *J. Comp. Neurol.* 229, 233–241.

Jones, B. E. (2005). From waking to sleeping: neuronal and chemical substrates. *Trends Pharmacol. Sci.* 26, 578–586.

Khateb, A., Fort, P., Pegna, A., Jones, B. E., and Mühlethaler, M. (1995). Cholinergic nucleus basalis neurons are excited by histamine in vitro. *Neuroscience* 69, 495–506.

Koyama, Y., and Sakai, K. (2000). Modulation of presumed cholinergic mesopontine tegmental neurons by acetylcholine and monoamines applied iontophoretically in unanesthetized cats. *Neuroscience* 96, 723–733.

Lin, J. S. (2000). Brain structures and mechanisms involved in the control of cortical activation and wakefulness, with emphasis on the posterior hypothalamus and histaminergic neurons. *Sleep Med. Rev.* 4, 471–503.

Lin, J. S., Hou, Y., Sakai, K., and Jouvet, M. (1996). Histaminergic descending inputs to the mesopontine tegmentum and their role in the control of cortical activation and wakefulness in the cat. *J. Neurosci.* 16, 1523–1537.

Liu, Y. W., Li, J., and Ye, J. H., Histamine regulates activities of neurons in the ventrolateral preoptic nucleus, *J. Physiol.*, 2010, in press.

McCormick, D. A., and Williamson, A. (1989). Convergence and divergence of neurotransmitter action in human cerebral cortex. *Proc. Natl. Acad. Sci. U.S.A.* 86, 8098–8102.

McCormick, D. A., and Williamson, A. (1991). Modulation of neuronal firing mode in cat and guinea pig LGNd by histamine: possible cellular mechanisms of histaminergic control of arousal. *J. Neurosci.* 11, 3188–3199.

Monti, J. M. (1993). Involvement of histamine in the control of the waking state. *Life Sci.* 53, 1331–1338.

Ohtsu, H., Tanaka, S., Terui, T., Hori, Y., Makabe-Kobayashi, Y., Pejler, G., Buzas, E., Kovacs, P., Csaba, G., Kittel, A., Okada, M., Hara, M., Mar, L., Numayama-Tsuruta, K., Ishigaki-Suzuki, S., Ohuchi, K., Ichikawa, A., Falus, A., Watanabe, T., and Nagy, A. (2001). Mice lacking histidine decarboxylase exhibit abnormal mast cells. *FEBS Lett.* 502, 53–56.

Paladini, C., Beckstead, M. J., and Weinshenker, D. (2007). Electrophysiological properties of catecholaminergic neurons in the norepinephrine-deficient mouse. *Neuroscience* 144, 1067–1074.

Panula, P., Yang, H. Y., and Costa, E. (1984). Histamine-containing neurons in the rat hypothalamus. *Proc. Natl. Acad. Sci. U.S.A.* 81, 2572–2576.

Parmentier, R., Ohtsu, H., Djebbara-Hannas, Z., Valatx, J. L., Watanabe, T., and Lin, J. S. (2002). Anatomical, physiological, and pharmacological characteristics of histidine decarboxylase knock-out mice: evidence for the role of brain histamine in behavioral and sleep–wake control. *J. Neurosci.* 22, 7695–7711.

Sakai, K., and Crochet, S. (2000). Serotonergic dorsal raphe neurons cease firing by disfacilitation during paradoxical sleep. *Neuroreport* 11, 3237–3241.

Sakai, K., El Mansari, M., Lin, J. S., Zhang, J. G., and Vanni-Mercier, G. (1990). "The posterior hypothalamus in the regulation of wakefulness and paradoxical sleep," in *The Diencephalon and Sleep*, eds M. Mancia and G. Marini (New York, NY: Raven Press), 171–198.

Saper, C. B., Scammel, T. E., and Lu, J. (2005). Hypothalamic regulation of sleep and circadian rhythms. *Nature* 437, 1257–1263.

Schwartz, J. C., Arrang, J. M., Garbarg, M., Pollard, H., and Ruat, M. (1991). Histaminergic transmission in the mammalian brain. *Physiol. Rev.* 71, 1–51.

Senba, E., Daddona, T., Watanabe, T., Wu, J.-Y., and Nagy, J. L. (1985). Coexistence of adenosine deaminase, histidine decarboxylase and glutamate decarboxylase in hypothalamic neurons of the rat. *J. Neurosci.* 5, 3393–3402.

Staines, W. A., Yamamoto, T., Daddona, P. E., and Nagy, J. I. (1986). Neuronal colocalization of adenosine deaminase, monoamine oxidase, galanin and 5-hydroxytryptophan uptake in the tuberomamillary nucleus of the rat. *Brain Res. Bull.* 17, 351–365.

Szymusiak, R., Gvilia, I., and McGinty, D. (2007). Hypothalamic control of sleep. *Sleep Med.* 8, 291–301.

Takahashi, K., Kayama, Y., Lin, J. S., and Sakai, K. (2010). Locus coeruleus neuronal activity during the sleep-waking cycle in mice. *Neuroscience* 169, 1115–1126.

Takahashi, K., Lin, J. S., and Sakai, K. (2006). Neuronal activity of histaminergic tuberomammillary neurons during wake–sleep states in the mouse. *J. Neurosci.* 26, 10292–10298.

Takahashi, K., Lin, J. S., and Sakai, K. (2008). Neuronal activity of orexin and non-orexin waking-active neurons during wake–sleep states in the mouse. *Neuroscience* 153, 860–870.

Takahashi, K., Lin, J. S., and Sakai, K. (2009). Characterization and mapping of sleep-waking specific neurons in the basal forebrain and preoptic hypothalamus in mice. *Neuroscience* 161, 269–292.

Takeda, N., Inagaki, S., Shiosaka, S., Taguchi, Y., Oertel, W. H., Tohyama, M., Watanabe, T., and Wada, H. (1984). Immunohistochemical evidence for the coexistence of histidine decarboxylase-like and glutamate decarboxylase-like immunoreactivities in nerve cells of the magnocellular nucleus of the posterior hypothalamus of rats. *Proc. Natl. Acad. Sci. U.S.A.* 81, 7647–7650.

Vincent, S. R., Hökfelt, T., Skirboll, L. R., and Wu, J. Y. (1983). Hypothalamic gamma-aminobutyric acid neurons project to the cortex. *Science* 220, 1309–1311.

Wada, H., Inagaki, N., Yamatodani, A., and Watanabe, T. (1991). Is the histaminergic neuron system a regulatory center for whole-brain activity? *Trends Neurosci.* 14, 415–418.

Watanabe, T., Taguchi, Y., Shiosaka, S., Tanaka, J., Kubota, H., Terano, Y., Tohyama, M., and Wada, H. (1984). Distribution of the histaminergic neuron system in the central nervous system of rats; a fluorescent immuno-histochemical analysis with histidine decarboxylase as a marker. *Brain Res.* 295, 13–25.

Yanai, K., and Tashiro, M. (2007). The physiological and pathophysiological roles of neuronal histamine: an insight from human positron emission tomography studies. *Pharmacol. Ther.* 113, 1–15.